AMERICAN SOCIETY FOR MICROBIOLOGY | Journal of Virology®

VACCINES AND ANTIVIRAL AGENTS

High-Throughput Screening and Identification of Potent Broad-Spectrum Inhibitors of Coronaviruses

Liang Shen,[a] Junwei Niu,[a] Chunhua Wang,[b] Baoying Huang,[a] Wenling Wang,[a] Na Zhu,[a] Yao Deng,[a] Huijuan Wang,[a] Fei Ye,[a] Shan Cen,[c] Wenjie Tan[a]

[a]NHC Key Laboratory of Biosafety, Ministry of Health, National Institute for Viral Disease Control and Prevention, China CDC, Beijing, China
[b]National Institutes for Food and Drug Control, Beijing, China
[c]Department of Immunology, Institute of Medicinal Biotechnology, Chinese Academy of Medical Sciences, Beijing, China

ABSTRACT Coronaviruses (CoVs) act as cross-species viruses and have the potential to spread rapidly into new host species and cause epidemic diseases. Despite the severe public health threat of severe acute respiratory syndrome coronavirus and Middle East respiratory syndrome CoV (MERS-CoV), there are currently no drugs available for their treatment; therefore, broad-spectrum inhibitors of emerging and endemic CoVs are urgently needed. To search for effective inhibitory agents, we performed high-throughput screening (HTS) of a 2,000-compound library of approved drugs and pharmacologically active compounds using the established genetically engineered human CoV OC43 (HCoV-OC43) strain expressing *Renilla* luciferase (rOC43-ns2Del-Rluc) and validated the inhibitors using multiple genetically distinct CoVs *in vitro*. We screened 56 hits from the HTS data and validated 36 compounds *in vitro* using wild-type HCoV-OC43. Furthermore, we identified seven compounds (lycorine, emetine, monensin sodium, mycophenolate mofetil, mycophenolic acid, phenazopyridine, and pyrvinium pamoate) as broad-spectrum inhibitors according to their strong inhibition of replication by four CoVs *in vitro* at low-micromolar concentrations. Additionally, we found that emetine blocked MERS-CoV entry according to pseudovirus entry assays and that lycorine protected BALB/c mice against HCoV-OC43-induced lethality by decreasing viral load in the central nervous system. This represents the first demonstration of *in vivo* real-time bioluminescence imaging to monitor the effect of lycorine on the spread and distribution of HCoV-OC43 in a mouse model. These results offer critical information supporting the development of an effective therapeutic strategy against CoV infection.

IMPORTANCE Currently, there is no approved therapy to treat coronavirus infection; therefore, broad-spectrum inhibitors of emerging and endemic CoVs are needed. Based on our high-throughput screening assay using a compound library, we identified seven compounds with broad-spectrum efficacy against the replication of four CoVs *in vitro*. Additionally, one compound (lycorine) was found to protect BALB/c mice against HCoV-OC43-induced lethality by decreasing viral load in the central nervous system. This inhibitor might offer promising therapeutic possibilities for combatting novel CoV infections in the future.

KEYWORDS Coronaviruses, bioluminescence imaging, broad-spectrum, high-throughput screening, inhibitor, mice

Emerging viruses are difficult to control, because they periodically cycle in and out of humans and livestock; therefore, effective vaccines and antivirals are urgently needed. Coronaviruses (CoVs) represent a group of enveloped, positive-sense, single-stranded viruses with large genomes (27 to 33 kb) and capable of causing respiratory, enteric, hepatic, and neurological diseases of differing severities in diverse animal

Citation Shen L, Niu J, Wang C, Huang B, Wang W, Zhu N, Deng Y, Wang H, Ye F, Cen S, Tan W. 2019. High-throughput screening and identification of potent broad-spectrum inhibitors of coronaviruses. J Virol 93:e00023-19. https://doi.org/10.1128/JVI.00023-19.

Editor Tom Gallagher, Loyola University Chicago

Address correspondence to Wenjie Tan, tanwj28@163.com.

L.S. and J.N. contributed equally to this work.

Received 7 January 2019
Accepted 17 March 2019
Accepted manuscript posted online 27 March 2019
Published 29 May 2019

species, including humans. All CoVs have a similar genome organization: approximately two-thirds of the 5′-proximal genome contains the ORF1a/b replicase gene, and the remainder encodes the spike, envelope, membrane, and nucleocapsid structural proteins along with several accessory proteins. CoVs belong to the family *Coronaviridae* in the order *Nidovirales* (1) and are divided into four genera: alpha-, beta-, gamma-, and delta-CoVs. Only alpha- and beta-CoVs can infect humans, with four CoVs currently known to be prevalent: human CoV 229E (HCoV-229E), HCoV-OC43, HCoV-HKU1, and HCoV-NL63. Severe acute respiratory syndrome CoV (SARS-CoV) and Middle East respiratory syndrome CoV (MERS-CoV) (2, 3) are considered the most emergent CoVs.

CoV infections are difficult to prevent and cure. Although CoV replication machinery exhibits substantial proofreading activity, estimates of the nucleotide mutation rate in CoVs are moderate to high relative to that of other single-stranded RNA viruses. Additionally, the large RNA genome in CoVs allows for extra plasticity in genome modification by recombination (4–6). Moreover, many animal CoVs cause long-term or persistent enzootic infections, which increase the probability of infecting a new host species. SARS-CoV and MERS-CoV are recent examples of newly emergent CoVs that cause severe human diseases (7, 8). Several drugs, such as ribavirin, lopinavir-ritonavir, interferon, and corticosteroids, have been used to treat patients infected with SARS-CoV or MERS-CoV (9–12). However, contradictory findings on their efficacy and concerns over tolerability and clinical benefit have limited the use of antiviral therapeutics for CoVs. Although substantial effort has focused on identifying antivirals for CoV treatment, no approved therapeutic (drug or biological agent) is currently available for the prophylaxis or treatment of CoV-related disease. Treatments for emerging CoV diseases rely upon supportive care and the judicious use of limited quantities of experimental therapeutics (13). Moreover, the lack of effective drugs, the high morbidity and mortality rates caused by the virus, and the potential of epidemic spread highlight the need for new broad-spectrum anti-CoV drugs, especially given the likelihood of infection by novel CoVs (13).

Several recent studies highlighted potential broad-spectrum inhibitors against CoVs (13–17). de Wilde et al. (14) identified numerous potent MERS-CoV inhibitors through screening of a U.S. Food and Drug Administration (FDA)-approved drug library. Interestingly, all of the screened compounds were also capable of inhibiting the replication of SARS-CoV and HCoV-229E. Dyall et al. (15) also screened 27 compounds with activity against both MERS-CoV and SARS-CoV from a 290-compound library; however, the half-maximal effective concentration (EC_{50}) values of most of these drugs were relatively high *in vitro* but were not assessed *in vivo,* making their clinical utility questionable. Müller et al. (16) found that silvestrol was a potent and nontoxic inhibitor of cap-dependent viral mRNA translation in CoV-infected human primary cells, with EC_{50} values of 1.3 nM and 3 nM for MERS-CoV and HCoV-229E, respectively. Notably, Sheahan et al. (17) showed that a nucleotide prodrug (GS-5734) could inhibit SARS-CoV and MERS-CoV replication in multiple *in vitro* systems at submicromolar half-maximal inhibitory concentration (IC_{50}) values. Furthermore, the prophylactic and early therapeutic administration of GS-5734 significantly reduced the lung viral load and improved clinical signs of disease, as well as respiratory function, in a mouse model of SARS-CoV pathogenesis, further supporting the development of GS-5734 as a broad-spectrum therapeutic to protect against CoVs.

HCoV-OC43, SARS-CoV, and MERS-CoV all belong to beta-CoVs and show a high degree of conservation of essential functional domains, especially within 3CLpro, RdRp, and the RNA helicase, which might represent potential targets for broad-spectrum anti-CoV drugs. We recently reported that a genetically engineered CoV strain (HCoV-OC43) expressing *Renilla* luciferase (Rluc; rOC43-ns2Del-Rluc) facilitates high-throughput screening (HTS) for broad-spectrum anti-CoV agents and quantitative analysis of CoV replication (18). In the present study, we performed HTS of a 2,000-compound library containing FDA-approved drugs and pharmacologically active compounds and assessed broad-spectrum anti-CoV activity *in vitro* and *in vivo* in an experimental infection mouse model. This comprehensive screening and assessment

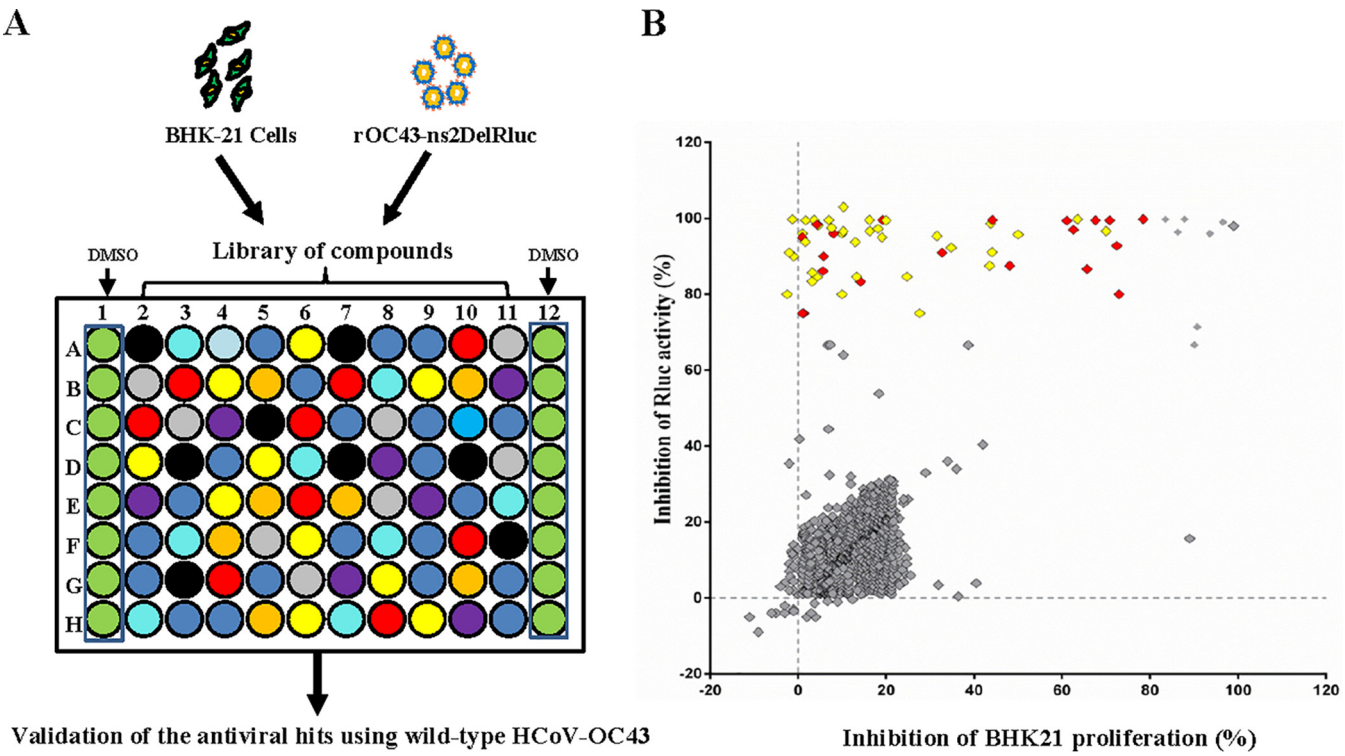

FIG 1 Screening for anti-HCoV-OC43 compounds. (A) Schematic of the HTS assay. BHK-21 cells were seeded in 96-well plates, and after a 24-h incubation (~10,000 cells/well), the medium was replaced with 94 μl DMEM supplemented with 3% FBS. The cells were treated in triplicate with 1 μl of each compound (diluted in DMSO) at a final concentration of 10 μM. After 1 h, 5 μl of rOC43-ns2Del-Rluc was added, and the cells were cultured for an additional 72 h, after which Rluc activity, represented as relative light units (RLUs), was measured. Screened compounds were confirmed using HCoV-OC43-WT. (B) Overview of HTS and the confirmation assay. All compounds and their corresponding activity are represented by squares. The percentage inhibition of Rluc activity of rOC43-ns2Del-Rluc is displayed along the vertical axis versus the percentage inhibition of BHK-21 proliferation displayed along the horizontal axis. Compounds exhibiting >70% inhibition of Rluc activity and <80% cytotoxicity were considered effective inhibitors of rOC43-ns2Del-Rluc and are displayed in red and yellow (yellow squares represent the compounds screened in the HTS using rOC43-ns2Del-Rluc and confirmed using HCoV-OC43-WT), with the ineffective compounds displayed in gray. Data represent the mean ± standard deviation of the results of three replicates. The screening assay was repeated at least three times.

provided new candidate inhibitors to effectively treat infections by existing CoVs, as well as those by emergent strains in the future.

RESULTS

HTS of anti-HCoV-OC43 compounds. Optimal screening conditions were established using the rOC43-ns2Del-Rluc reporter virus to infect BHK-21 cells in 96-well plates (multiplicity of infection [MOI] = 0.01; 10,000 cells/well). Under this condition, the coefficient of variation and Z factor were 2.9% and 0.86, respectively, demonstrating that the assay was robust and suitable for HTS.

A schematic of the HTS strategy is depicted in Fig. 1A. In the primary screening from the 2,000-compound library under a concentration of 10 μM, 56 hits were found to significantly inhibit rOC43-ns2Del-Rluc replication (Fig. 1B, red and yellow squares), with ≥70% reduced Rluc activity and ≤80% cytotoxicity, including 12 FDA-approved drugs. To obtain more potent inhibitors and exclude the possibility that the observed antiviral activity was specific to rOC43-ns2Del-Rluc, we confirmed the antiviral activity of the 56 hits against wild-type HCoV-OC43 (HCoV-OC43-WT) by quantitative reverse transcription (qRT)-PCR under a lower concentration (5 μM), which confirmed the antiviral activity of 36 compounds (Fig. 1B, yellow squares).

Identification of broad-spectrum anti-CoV inhibitors *in vitro*. Because only alpha- and beta-CoVs infect humans, we focused on three other CoVs (MERS-CoV [beta-CoV], mouse hepatitis virus A59 [MHV-A59] [beta-CoV], and HCoV-NL63 [alpha-CoV]) to assess the broad-spectrum antiviral activity of the 36 compounds by using an eight-point dose-response confirmation (15). We identified 17 compounds that inhib-

TABLE 1 Properties and antiviral activities of 36 compounds against four CoVs

Compound name[a]	CAS no.	Formula	Bioactivity[b]	HCoV-OC43 EC_{50}, CC_{50}	HCoV-NL63 EC_{50}, CC_{50}	MERS-CoV EC_{50}, CC_{50}	MHV-A59 EC_{50}, CC_{50}
Lycorine	476-28-8	$C_{16}H_{17}NO_4$	Inhibits cell division, antineoplastic, antiviral	0.15, 4.37	0.47, 3.81	1.63, 3.14	0.31, 3.51
Emetine	483-18-1	$C_{29}H_{42}C_{l2}N_2O_4$	Inhibits RNA, DNA, and protein synthesis	0.30, 2.69	1.43, 3.63	0.34, 3.08	0.12, 3.51
Mycophenolate mofetil	115007-34-6	$C_{23}H_{31}NO_7$	Immune suppressant, antineoplastic, antiviral	1.58, 3.43	0.23, 3.01	1.54, 3.17	0.27, 3.33
Phenazopyridine	94-78-0	$C_{11}H_{12}ClN_5$	Analgesic	1.90, >20	2.02, >20	1.93, >20	0.77, >20
Mycophenolic acid	24280-93-1	$C_{17}H_{20}O_6$	Immune suppressant, antineoplastic, antiviral	1.95, 3.55	0.18, 3.44	1.95, 3.21	0.17, 4.18
Pyrvinium pamoate	3546-41-6	$C_{49}H_{43}N_3O_6$	Anthelmintic	3.21, >20	3.35, >20	1.84, 19.91	4.12, 19.98
Monensin sodium	22373-78-0	$C_{37}H_{63}NaO_{10}$	Antibacterial	3.81, >20	1.54, >20	3.27, >20	0.18, >20
Cycloheximide	66-81-9	$C_{15}H_{23}NO_4$	Protein synthesis inhibitor	0.43, 3.12	2.64, 3.24	2.56, 2.96	5.21, 3.19
Cetylpyridinium chloride	6004-24-6	$C_{21}H_{38}ClN$	Anti-infective	4.31, 8.23	1.24, 8.52	0.69, 8.14	7.86, 8.19
Oligomycin	1404-19-9	$C_{45}H_{74}O_{11}$	Antibacterial, antifungal	0.19, 6.56	2.63, 4.26	0.21, 5.16	6.43, 6.78
Promazine	58-40-2	$C_{17}H_{21}ClN_2S$	Antipsychotic	0.41, >20	1.37, >20	13.72, >20	0.51, >20
Diperodon	537-12-2	$C_{22}H_{28}ClN_3O_4$	Analgesic, anesthetic	1.71, 14.3	4.91, 13.6	8.77, 14.2	1.98, 14.5
Dihydrocelastryl diacetate	None	$C_{33}H_{44}O_6$	Antibacterial	1.71, >20	0.65, >20	10.58, >20	4.24, >20
Tetrandrine	518-34-3	$C_{38}H_{42}N_2O_6$	Analgesic, antineoplastic, antihypertensive	0.29, >20	2.05, >20	12.68, >20	4.81, >20
Pristimerin	1258-84-0	$C_{30}H_{40}O_4$	Antineoplastic, anti-inflammatory	1.99, >20	1.63, >20	13.87, >20	9.17, >20
Chloroquine	54-05-7	$C_{18}H_{32}ClN_3O_8P_2$	Antimalarial, antiamebic, antirheumatic	0.33, >20	4.89, >20	16.44, >20	15.92, >20
Valinomycin	2001-95-8	$C_{54}H_{90}N_6O_{18}$	Antibiotic	4.43, 6.15	1.89, 4.12	6.07, 5.88	6.78, 5.11
Loperamide	34552-83-5	$C_{29}H_{34}Cl_2N_2O_2$	Ca channel blocker	1.86, 18.7	6.47, 18.27	4.82, 18.9	10.65, 18.9
Harmine	442-51-3	$C_{13}H_{12}N_2O$	Antiparkinsonian, CNS stimulant	1.90, >20	13.46, >20	4.93, >20	13.77, >20
Conessine	546-06-5	$C_{24}H_{40}N_2$	Antimalarial, antihistamine	2.34, >20	10.75, >20	4.98, >20	11.46, >20
Chloropyramine	6170-42-9	$C_{16}H_{21}Cl_2N_3$	Antihistamine	1.79, >20	14.21, >20	14.21, >20	2.42, >20
Doxazosin mesylate	77883-43-3	$C_{24}H_{29}N_5O_8S$	Antihypertensive	4.97, >20	13.95, >20	12.66, >20	14.48, >20
Alprenolol	13655-52-2	$C_{15}H_{24}ClNO_2$	Beta-adrenergic blocker	1.95, >20	11.88, >20	10.53, >20	13.97, >20
Berbamine	478-61-5	$C_{37}H_{42}Cl_2N_2O_6$	Antihypertensive, skeletal muscle relaxant	1.48, >20	9.46, >20	13.14, >20	10.91, >20
Phenylmercuric acetate	62-38-4	$C_8H_8HgO_2$	Antifungal	2.17, 5.35	6.79, 5.47	6.44, 5.39	6.81, 5.97
Hycanthone	3105-97-3	$C_{20}H_{24}N_2O_2S$	Anthelmintic, hepatotoxic	0.16, 3.58	5.76, 3.68	5.11, 4.32	5.78, 4.19
Zoxazolamine	61-80-3	$C_7H_5ClN_2O$	Muscle relaxant, antirheumatic	1.39, >20	13.51, >20	14.21, >20	16.45, >20
Ticlopidine	53885-35-1	$C_{14}H_{15}Cl_2NS$	PAF inhibitor	1.41, >20	15.65, >20	11.25, >20	14.28, >20
4′-Hydroxychalcone	2657-25-2	$C_{15}H_{12}O_2$	Antineoplastic	1.52, >20	7.25, >20	10.23, >20	9.75, >20
Papaverine	61-25-6	$C_{20}H_{22}ClNO_4$	Muscle relaxant, cerebral vasodilator	1.61, 12.11	7.32, 11.71	9.45, 11.98	11.46, 12.44
Propranolol	318-98-9	$C_{16}H_{22}ClNO_2$	Antihypertensive, antianginal, antiarrhythmic	0.48, >20	8.11, >20	11.01, >20	13.54, >20
Tilorone	27591-69-1	$C_{25}H_{34}N_2O_3$	Antiviral	0.32, >20	6.89, >20	10.56, >20	16.11, >20
Antimycin A	1397-94-0	$C_{27}H_{38}N_2O_9$	Antifungal, antiviral, interferes in cytochrome oxidation	1.65, 3.62	6.05, 4.21	6.89, 4.32	5.42, 3.98
Salinomycin sodium	53003-10-4	$C_{42}H_{69}NaO_{11}$	Antibacterial	0.29, 1.97	5.71, 2.41	5.49, 3.84	5.16, 2.45
Exalamide	53370-90-4	$C_{13}H_{19}NO_2$	Antifungal	1.48, >20	17.49, >20	15.91, >20	16.39, >20
Desipramine	50-47-5	$C_{18}H_{23}ClN_2$	Antidepressant	1.67, >20	6.68, >20	11.59, >20	8.75, >20

[a]The compounds in bold inhibited the replication of all CoVs with EC_{50} values of <5 μM.
[b]CNS, central nervous system; PAF, platelet-activating factor.

ited the replication of HCoV-NL63 ($EC_{50} < 5$ μM), which is an alpha-CoV that usually causes the common cold, whereas 13 and 12 compounds inhibited MERS-CoV and MHV-A59 replication ($EC_{50} < 5$ μM), respectively (Table 1). Moreover, we newly identified nine compounds (phenazopyridine, lycorine, pyrvinium pamoate, monensin sodium, cetylpyridinium chloride, oligomycin, loperamide, harmine, and conessine) as exhibiting antiviral activity against severe CoV (MERS-CoV) (Table 1). Interestingly, the following seven compounds inhibited the replication of all CoVs with EC_{50} values of <5 μM: lycorine, emetine, phenazopyridine, mycophenolic acid, mycophenolate mofetil, pyrvinium pamoate, and monensin sodium (Table 1, compounds indicated in bold).

These seven broad-spectrum inhibitors suppressed the replication of all CoVs in a dose-dependent manner and with low EC_{50} values (Fig. 2). Lycorine, an active alkaloid from the common folk medicine *Lycoris radiata* (*Amaryllidaceae*) has been investigated for its multifunctional biological effects, including anticancer, antimalarial, antiviral, antibacterial, and anti-inflammatory activities (19–23). Lycorine showed potent anti-CoV activity, with EC_{50} values ranging from 0.15 μM to 1.63 μM. Moreover, the selective index (SI) of lycorine for HCoV-OC43 was calculated at 29.13, indicating its potent

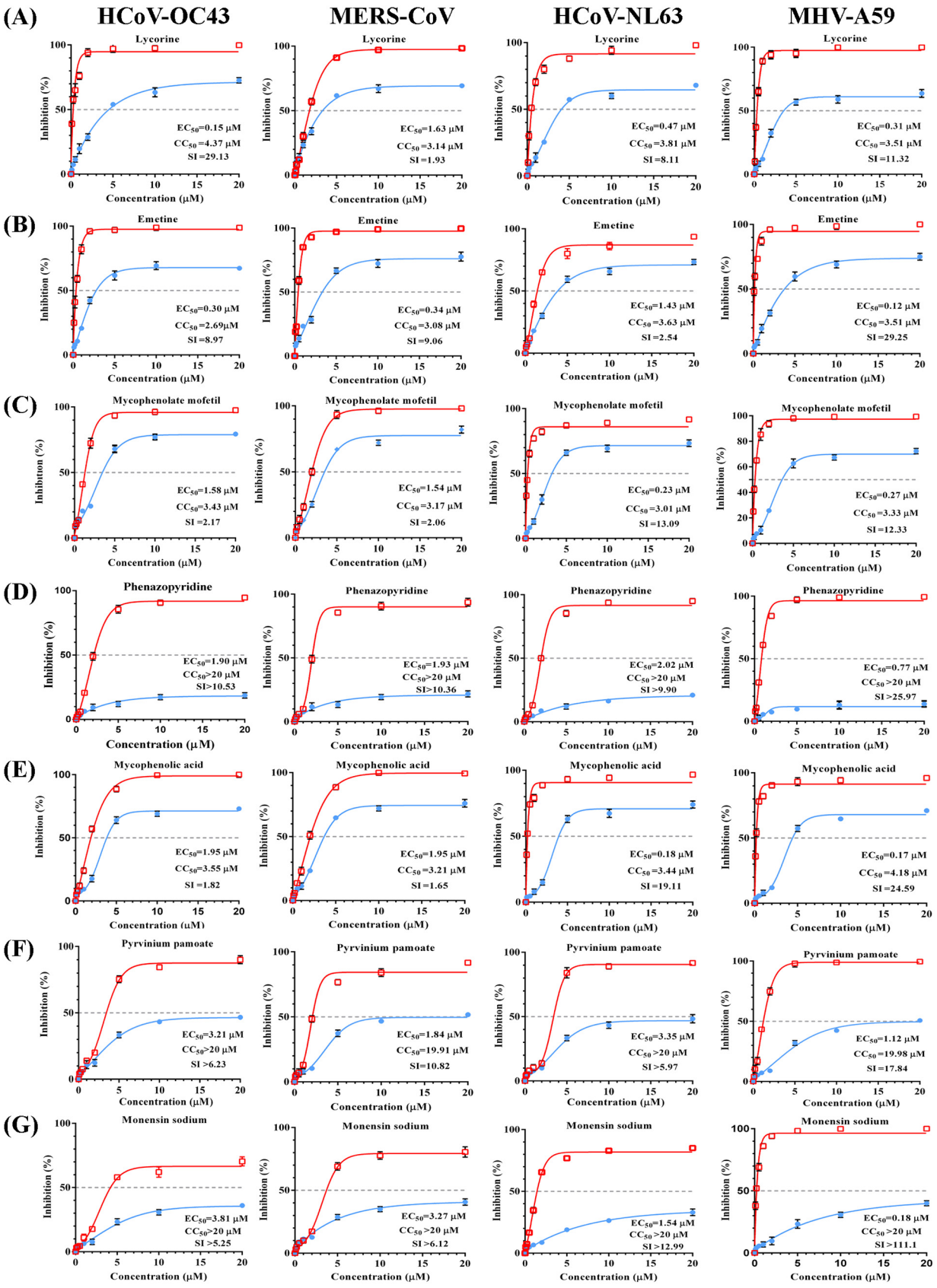

FIG 2 Dose-response curves for seven broad-spectrum inhibitors of four types of CoVs *in vitro*. BHK-21, Vero E6, LLC-MK2, or DBT cells were infected with HCoV-OC43-WT, MERS-CoV, HCoV-NL63, or MHV-A59 at an MOI of 0.01, respectively, and treated for 72 h with eight doses (0.1, 0.25, 0.5, 1,

(Continued on next page)

anti-HCoV-OC43 activity (Fig. 2A). Emetine is an active principal of ipecac and inhibits the replication of both DNA and RNA viruses. Additionally, emetine displayed potent anti-CoV activity and the strongest anti-MERS-CoV activity among the top seven inhibitors, with an EC_{50} value of 0.34 μM and an SI of 9.06 (Fig. 2B). Mycophenolic acid (an immunosuppressant) exerted a significant inhibitory effect on HCoV-OC43 replication, with an EC_{50} of 1.95 μM, and showed stronger anti-HCoV-NL63 activity than the others (EC_{50} of 0.18 μM and SI of 19.11) (Fig. 2E). Mycophenolate mofetil, a derivative of mycophenolic acid, showed an antiviral effect on the four CoVs similar to that of mycophenolic acid, suggesting that the two drugs might harbor similar core structures and antiviral mechanisms (Fig. 2C and E). Moreover, phenazopyridine, a widely used urinary analgesic, also displayed strong broad-spectrum anti-CoV activity for the first time, especially against MHV-A59 (EC_{50} of 0.77 μM and SI of $>$25.97) (Fig. 2D). Pyrvinium pamoate is an FDA-approved anthelminthic drug and a potent inhibitor of WNT signaling, suggested to occur through direct activation of protein kinase CK1α (24). Pyrvinium pamoate inhibited the replication of all CoVs and displayed low toxicity (50% cytotoxic concentration [CC_{50}], $>$19 μM) (Fig. 2F). Finally, monensin sodium, previously shown to inhibit the formation of gamma-CoV infectious bronchitis virus (IBV), inhibited all CoVs at low EC_{50} values and displayed low toxicity (Fig. 2G). Although the specific antiviral mechanisms of these seven inhibitors against CoVs are unknown, they showed potential as new antivirals for the treatment of infections caused by a range of CoVs.

Validation of anti-CoV activity. We verified the antiviral activity of the seven inhibitors against HCoV-OC43 by indirect immunofluorescence assay (IFA) and Western blot analysis. As shown in Fig. 3A, all seven inhibitors significantly suppressed HCoV-OC43 replication, compared with that of the control (dimethyl sulfoxide [DMSO]), and with a $>$90% inhibitory effect for most compounds, except for monensin sodium. Additionally, we observed inhibitory activity when the cells were treated with the inhibitors after viral infection, resulting in significantly reduced levels of HCoV-OC43 nucleocapsid protein (Fig. 3B). Although the inhibitory effect of mycophenolic acid differed according to IFA and Western blot results, the seven inhibitors clearly suppressed HCoV-OC43 replication.

Emetine inhibited MERS-CoV entry. Viral entry is an essential step of the viral life cycle and is thus an attractive target for therapy. Inhibition of this step can block viral propagation at an early stage of infection, thereby minimizing the chance for the virus to evolve and acquire drug resistance. Therefore, we tested the effect of the seven screened inhibitors on CoV entry using a pseudotype virus with a human immunodeficiency virus type 1 (HIV-1) backbone but expressing the spike protein of MERS-CoV in order to generate dose-response curves. Measurement of the inhibition percentage showed that only emetine was an entry inhibitor that blocked MERS-CoV S-mediated infection, with luciferase activity reduced 50-fold compared with that of the control and an EC_{50} value of 0.16 μM (Fig. 4).

Antiviral activity of lycorine against lethal HCoV-OC43 infection *in vivo*. HCoV-OC43 infects neurons and causes encephalitis in mice, with this model previously used for anti-CoV drug evaluation (25). Moreover, this model was convenient based on the lack of need for three biological facilities, in contrast to experiments involving SARS-CoV or MERS-CoV. Therefore, we used this model to evaluate the *in vivo* antiviral activity of the seven inhibitors. Intracerebral or intranasal inoculation of HCoV-OC43 results in acute-onset severe neurological illness and causes death, with high levels of viral replication in the brain (titer, $>10^6$ 50% tissue culture infective doses [$TCID_{50}$]/ml) at 3

FIG 2 Legend (Continued)
2, 5, 10, or 20 μM) of lycorine (A), emetine (B), mycophenolate mofetil (C), phenazopyridine (D), mycophenolic acid (E), pyrvinium pamoate (F), or monensin sodium (G). At 72 h postinfection, the cell culture supernatants were subjected to a viral load assay, and cell lysates were assessed for cytotoxicity. Percent inhibition was calculated as follows: inhibition of viral load (%) = 100% − [viral load (titers or copies) of each CoV in the compound-treated cells/viral load of DMSO-treated control cells]. Inhibition is shown in red, and cytotoxicity is shown in blue. EC_{50} values and SI (CC_{50}/EC_{50}) are shown. Data represent the mean ± standard deviation (error bars) of the results of three independent experiments.

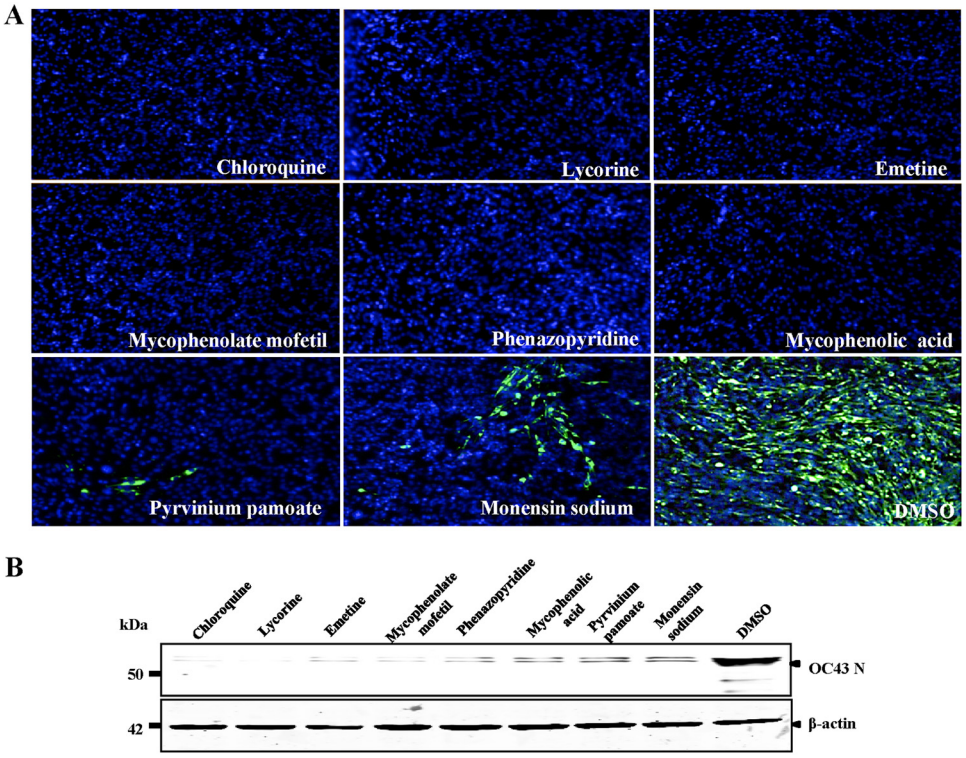

FIG 3 Confirmation of anti-CoV activity by IFA and Western blot analysis. (A) IFA of the HCoV-OC43 nucleocapsid (N) protein in inhibitor-treated BHK-21 cells. BHK-21 cells in 96-well plates were infected with HCoV-OC43-WT (MOI = 0.01) in the presence of 10 μM the indicated inhibitors, with chloroquine and DMSO used as the positive and negative controls, respectively. At 72 h postinfection, the cells were analyzed by IFA for N protein (green) expression. Nuclei (blue) were stained with DAPI. (B) The effect of the inhibitors on N protein synthesis by HCoV-OC43-WT was determined by Western blot analysis. BHK-21 cells in 12-well plates were infected with HCoV-OC43-WT (MOI = 0.01) in the presence of 10 μM the indicated inhibitors, with chloroquine and DMSO used as the positive and negative controls, respectively. At 72 h postinfection, cells were analyzed by Western blotting using antibodies against HCoV-OC43 N protein and β-actin.

to 5 days after infection (26–29). Briefly, female BALB/c mice (12 days old) were inoculated via the intranasal route with 100 $TCID_{50}$ of HCoV-OC43-WT and treated with the seven inhibitors for 14 days, and their survival was monitored for up to 20 days. The inhibitor doses and regimens were selected based on acute-toxicity assessments. Emetine was used at 5 mg/kg, and chloroquine was used as the positive control, which showed antiviral activity at 30 mg/kg. All mice in the phosphate-buffered saline (PBS)-DMSO-treated group died within 6 days after HCoV-OC43-WT challenge (Fig. 5A). In contrast, 83.3% of mice in the lycorine-treated group were still alive at 20 days postinoculation ($P < 0.001$), similar to the survival rate of the chloroquine-treated group (Fig. 5A). Additionally, viral loads in the brain and spinal cord were under the limit of detection in the lycorine-treated group (Fig. 5B), and immunohistochemistry (IHC) of mouse brain coronal sections showed that HCoV-OC43 nucleocapsid protein was present only in the PBS-DMSO-treated group, not in the lycorine-treated group (Fig. 5C).

Lycorine blocked the spread of rOC43-ns2Del-Rluc in the mouse brain. To more closely monitor the effect of lycorine on the spread and replication of HCoV-OC43 in the mouse central nervous system in real time, we used bioluminescence imaging (BLI) based on its important advantages of an intrinsically low background signal and very high sensitivity for monitoring light emission *in vivo*. As expected, PBS-DMSO-treated mice showed gradually increasing signal intensity postinoculation, whereas no signal was detected in the brains of lycorine-treated mice (Fig. 6A). These observations were confirmed by the $\sim 2 \times 10^5$-fold-higher Rluc activity in the PBS-DMSO-treated mice

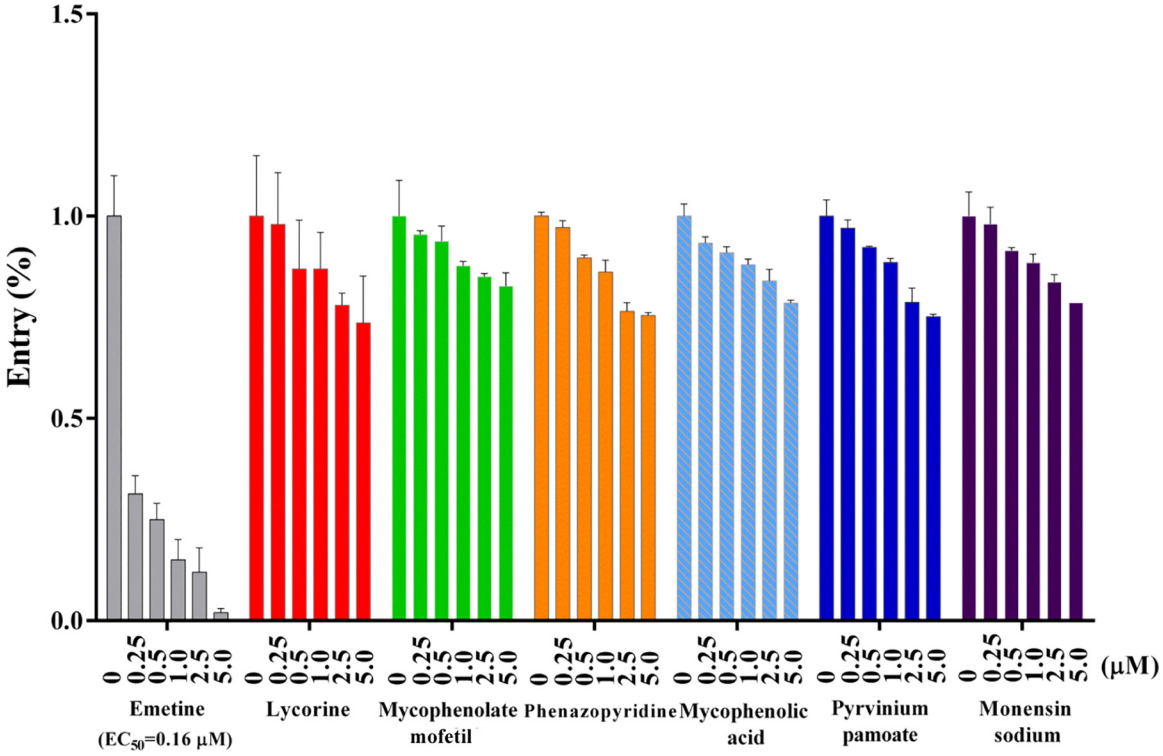

FIG 4 Emetine strongly inhibits MERS-CoV entry. DPP4-expressing Huh7.5 cells were cultured with 200 $TCID_{50}$ pseudotyped MERS-CoV in the presence of serial concentrations of individual inhibitors. The percentage of viral entry was calculated by measuring the luciferase expression of the inhibitor-treated cells relative to that in DMSO-treated cells. Data represent the mean ± standard deviation of the results of three replicates.

than in the lycorine-treated mice. Therefore, lycorine showed promise as an anti-CoV agent (Fig. 6B).

DISCUSSION

The SARS epidemic in 2003 and the ongoing MERS-CoV outbreak highlight the inadequacy of available treatments for life-threatening zoonotic CoV infections in humans. Indeed, no specific antiviral agent or vaccine is currently available for human or zoonotic CoV infections, despite the extensive research efforts triggered by the SARS outbreak (30–32). Several FDA-approved drugs (ritonavir, lopinavir, nelfinavir, mycophenolic acid, and ribavirin) inhibit the entry and/or replication of MERS-CoV, SARS-CoV, or other human CoVs in multiple cell lines; however, their antiviral efficacy *in vivo* remains unknown (16, 32–37). To date, few small molecules have demonstrated anti-CoV activity in animal models of CoV infection (17, 38, 39), and most of the available anti-CoV drugs that target structural proteins might not be effective against other CoVs. For example, the human monoclonal antibodies and antiviral peptides that block virus-host cell binding typically have a limited breadth of protection due to the antigenic diversity in the CoV spike glycoprotein (40, 41). It is worth mentioning that combining antiviral peptides with beta interferon (IFN-β) (40) or combination therapy with different humanized or human monoclonal antibodies targeting non-cross-resistant epitopes (42) can enhance antiviral therapeutic effects. There are also several reports of the enhanced therapeutic effects of combinations of other antiviral agents for the treatment of MERS-CoV. These results indicate that the combined use of different antiviral agents might be synergistic in their treatment of CoV infection.

Here, we identified seven potent broad-spectrum anti-CoV agents, among which lycorine was confirmed as showing strong anti-CoV activity *in vivo*. Our results suggest that FDA-approved drugs can be used for the prophylaxis of severe or lethal CoV

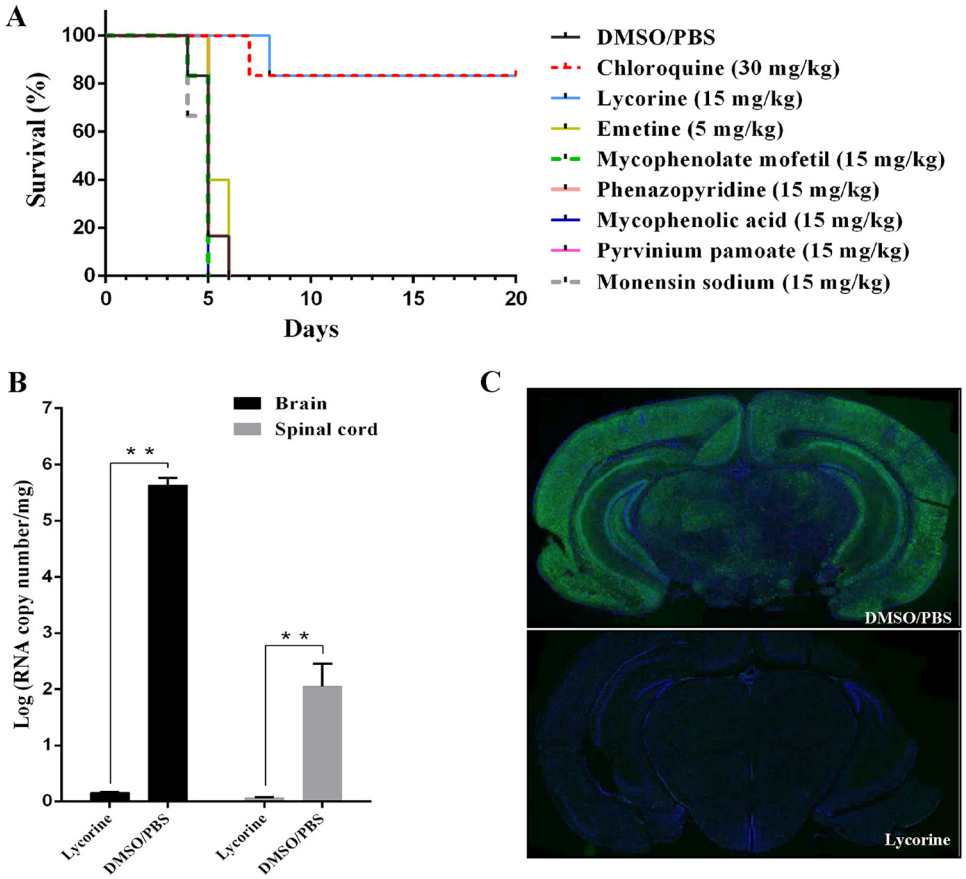

FIG 5 Lycorine protects mice against HCoV-OC43 infection. (A) Kaplan-Meier survival curves of mice >20 days after intranasal inoculation of HCoV-OC43, followed by treatment with the indicated inhibitors ($n = 6$/group). Inhibitor doses and regimens were selected based on their acute toxicity (emetine was used at 5 mg/kg, chloroquine was used at 30 mg/kg, and the other inhibitors were used at 15 mg/kg). (B) Viral loads in the mouse brain and spinal cord treated with lycorine. Twelve-day-old female BALB/c mice were inoculated via the intranasal route with 100 $TCID_{50}$ HCoV-OC43-WT and treated with lycorine or DMSO control for 3 days. At 72 h postinfection, viral loads in the mouse brain and spinal cord were determined by qRT-PCR. Data represent the mean ± standard deviation (error bars) of the results of three independent experiments. (C) IHC analyses of brain tissue from mice treated with lycorine. Twelve-day-old female BALB/c mice were inoculated via the intranasal route with 100 $TCID_{50}$ HCoV-OC43-WT and treated with lycorine or DMSO control for 3 days. Mouse brain coronal sections were stained for HCoV-OC43 N (green) and nuclei (blue).

infections, thereby greatly facilitating the rapid and rational development of anti-CoV agents with desirable pharmacokinetic and biodistribution properties.

The criteria for the inhibition rate associated with the signals in the antiviral HTS assay ranged from ~30% to ~90% according to different references, with more primary hits but fewer efficacy hits screened when the inhibition rate was set to the lower threshold. In our experiment, we focused on screening hits with higher potency and, therefore, so established the inhibition threshold at 70%. Furthermore, we identified several effective hits with a high degree of cytotoxicity under 10 μM in our primary screening, which was why the cytotoxicity value was set to 80%. Finally, we identified 36 compounds exhibiting anti-HCoV-OC43 activity from a library of compounds, two of which (chloroquine and loperamide) were previously reported as exhibiting broad-spectrum anti-CoV activity. Nine compounds (phenazopyridine, lycorine, pyrvinium pamoate, monensin sodium, cetylpyridinium chloride, oligomycin, loperamide, harmine, and conessine) have not previously been demonstrated as exhibiting antiviral activity against MERS-CoV, thereby offering new therapeutic possibilities for this severe CoV. Furthermore, seven compounds (lycorine, emetine, monensin sodium, mycophenolate mofetil, mycophenolic acid, phenazopyridine, and pyrvinium pamoate) showed inhib-

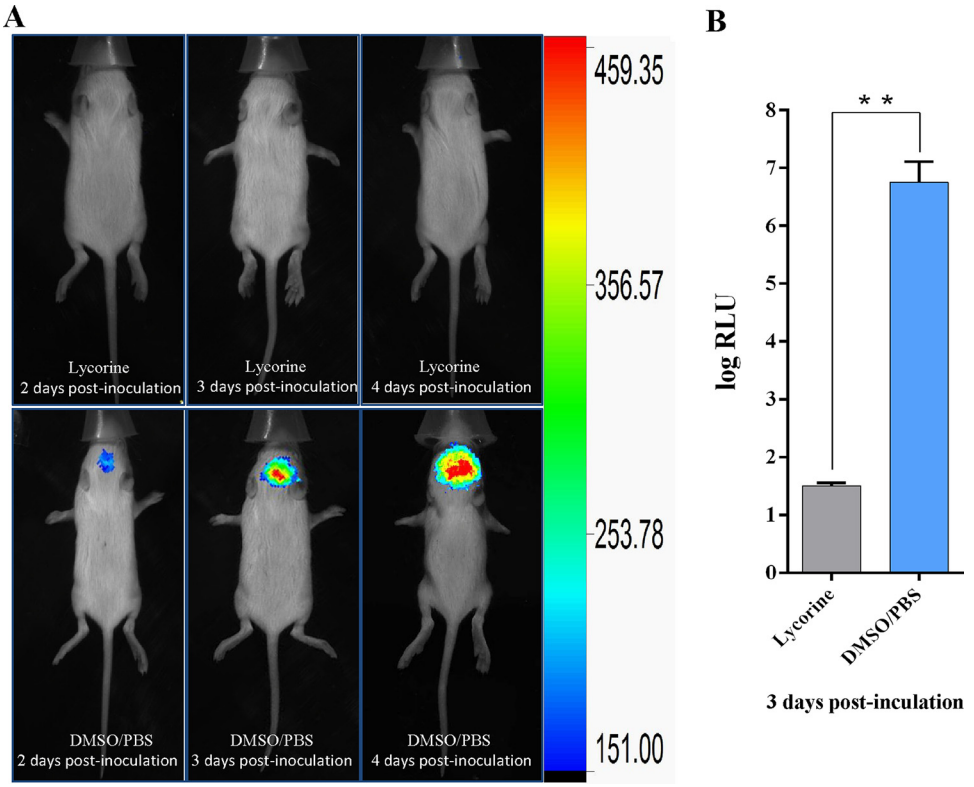

FIG 6 Lycorine inhibits the spread of rOC43-ns2Del-Rluc in the mouse brain. (A) Representative dorsal images of 12-day-old female BALB/c mice administered 15 mg/kg lycorine in DMSO-PBS or DMSO-PBS alone daily after inoculation with rOC43-ns2Del-Rluc. At 2, 3, and 4 days postinoculation, mice were processed for BLI, with the results are displayed as a heat map. (B) Rluc activity of rOC43-ns2Del-Rluc in the mouse brain at 72 h postinoculation. Data represent the mean ± standard deviation (error bars) of the results of three independent experiments. **, $P < 0.01$.

itory activity against multiple genetically distinct CoVs *in vitro* at low-micromolar concentrations (EC_{50} values ranging from 0.12 to 3.81 μM). Among these, lycorine is an alkaloid isolated from *Amaryllidaceae* plants and reportedly exhibits anticancer, antiplasmodial, antitrypanosomal, anti-inflammatory, analgesic, and emetic activities (43–45). Lycorine inhibits the replication of poliomyelitis virus, herpes simplex virus 1, Bunyamwera virus, West Nile virus, dengue virus, and SARS-CoV *in vitro,* although the mechanism remains to be elucidated (46–49). Liu et al. (50) demonstrated the ability of lycorine to reduce the mortality of human enterovirus 71-infected mice by inhibiting viral replication. Furthermore, Guo et al. (51) evaluated a total of 32 lycorine derivatives, demonstrating that 1-acetyllycorine suppressed enterovirus 71 and hepatitis C virus replication in various cells. Moreover, drug resistance analysis revealed that 1-acetyllycorine targeted a phenylalanine (F76) in the viral proteases. Lycorine also exhibits strong activities against influenza A virus H5H1 *in vitro* and delays the export of nucleoprotein from the nucleus to the cytoplasm during replication (52). However, the potential mechanism of lycorine against CoVs requires further exploration, and its potential selection for drug-resistant strains must be assessed. We found no reports concerning whether its use in combination enhances the antiviral efficacy of lycorine. Additionally, emetine is a drug used mainly as both an antiprotozoal and an emetic (53), with a number of groups recently reporting new antiviral roles for emetine. Emetine is reportedly a potent inhibitor that suppresses the replication of several RNA viruses (dengue virus and HIV) without generating drug-resistant variant viruses (54–56). We noted that emetine inhibits human cytomegalovirus (HCMV) replication by disrupting the HCMV-induced interaction between p53 and the E3-ubiquitin ligase MDM2 (57). Moreover, a recent study revealed emetine as an inhibitory modulator of rabies virus

axonal transport via a mechanism independent of protein synthesis inhibition (58). Furthermore, Yang et al. (59) demonstrated that emetine inhibits Zika virus (ZIKV) replication via inhibition of ZIKV NS5 polymerase activity and disruption of lysosomal function. In the present study, our preliminary result indicated that emetine inhibited MERS-CoV entry. Interestingly, the immunosuppressant mycophenolic acid and its derivative mycophenolate mofetil, which suppress MERS-CoV replication (33), also inhibited HCoV-OC43 replication (EC_{50} values of 1.95 and 1.58 μM, respectively). However, a previous study showed that MERS-CoV-infected common marmosets treated with mycophenolate mofetil had more severe forms of disease and higher lung viral loads than did untreated animals, and renal transplant recipients on maintenance mycophenolate mofetil therapy reportedly developed severe or fatal MERS (60). Therefore, these two inhibitors are unlikely to be useful against CoV infections. Monensin sodium, which affects IBV and MHV-A59 assembly (61, 62), was also identified as an inhibitor of other CoVs (MERS-CoV, HCoV-OC43, and HCov-NL63) in this study.

Lycorine showed strong antiviral activity against multiple genetically distinct CoVs *in vitro* and protected mice against lethal HCoV-OC43 infection *in vivo*. To our knowledge, this is the first report of the use of BLI to evaluate the effects of antiviral agents on CoV replication and dissemination *in vivo* without the need for sacrificing animals to quantify viral titers and establish the complete pattern of virus dissemination in the central nervous system. However, most of the data and conclusions concerning the antiviral effects of the inhibitors were derived only from one cell line and should be tested in different CoV replication cell lines in order to exclude the influence of host cell factors, especially for MERS-CoV, for which there are a larger number of susceptible cell lines (e.g., Huh 7 or Calu3/2B4 cells). Therefore, further *in vitro* and *in vivo* studies are warranted to determine the potential antiviral mechanisms associated with the seven compounds, as well as their clinical efficacy. Additionally, the efficacy of lycorine-interferon combinations should be explored in animal models.

Following SARS and MERS, future emerging CoVs will likely pose a threat to public health. Therefore, identification of broad-spectrum inhibitors of SARS-CoV, MERS-CoV, and future emerging CoVs is a research priority. From this perspective, the potent broad-spectrum inhibitors (lycorine and emetine) identified in this study might be effective against CoV infections either as single agents or in combination.

MATERIALS AND METHODS

Cell lines, viruses, compounds, and antibodies. BHK-21, Vero-E6, LLC-MK2, DBT, 293FT, DPP4-expressing Huh7.5 cells, and 17Cl-1 cells were cultured in Dulbecco's modified Eagle's medium (DMEM; Gibco, Thermo Fisher Scientific, Waltham, MA, USA) supplemented with 10% fetal bovine serum (FBS; Gibco) and incubated at 37°C in an atmosphere containing 5% CO_2.

HCoV-OC43 (GenBank accession number AY391777.1) expressing the Rluc gene (rOC43-ns2Del-Rluc) and derived from an infectious cDNA clone (17) was used for HTS in HBK-21 cells. HCoV-NL63 strain Amsterdam I was used to infect monolayers of LLC-MK2 cells at an MOI of 0.01. The MERS-CoV strain EMC was used to infect monolayers of Vero-E6 cells at an MOI of 0.01. The MHV strain A59 was propagated in 17Cl-1 cells, and a plaque assay was performed in monolayers of DBT cells infected with MHV at an MOI of 0.01.

A 2,000-compound library containing FDA-approved drugs and pharmacologically active compounds was purchased from MicroSource Discovery Systems, Inc. (Gaylordsville, CT, USA) (see Table S1 in the supplemental material).

The anti-HCoV-OC43 nucleocapsid protein mouse monoclonal antibody was made in-house. Anti-β-actin (13E5) rabbit monoclonal antibody was obtained from Cell Signaling Technology (Danvers, MA, USA). Infrared IRDye 800CW-labeled goat anti-mouse IgG and 680RD-labeled goat anti-rabbit IgG were purchased from LI-COR Biosciences (Lincoln, NE, USA).

Viral load assays. MHV titers were quantified by a plaque assay, as described previously (63). Viral genomic RNA from HCoV-OC43, HCoV-NL63, and MERS-CoV was extracted from 50 μl of cell culture supernatants using a QIAamp viral RNA minikit (Qiagen, Valencia, CA, USA) and quantified by real-time RT-PCR, as described previously (64, 65). The primer and probe sequences were as follows: q-OC43-F, 5′-GCT CAG GAA GGT CTG CTC C-3′; q-OC43-R, 5′-TCC TGC ACT AGA GGC TCT GC-3′; q-OC43-probe, 5′-FAM (6-carboxyfluorescein)-TTC CAG ATC TAC TTC GCG CAC ATC C-TAMRA (6-carboxytetramethylrhodamine)-3′; q-NL63-F, 5′-AGG ACC TTA AAT TCA GAC AAC GTT CT-3′; q-NL63-R, 5′-GAT TAC GTT TGC GAT TAC CAA GAC T-3′; q-NL63-probe, 5′-FAM-TAA CAG TTT TAG CAC CTT CCT TAG CAA CCC AAA CA-TAMRA-3′; q-MERS-F, 5′-GGC ACT GAG GAC CCA CGT T-3′, q-MERS-R, 5′-TTG CGA CAT ACC CAT AAA AGC A-3′; and q-MERS-probe, 5′-FAM-CCC CAA ATT GCT GAG CTT GCT CCT ACA-TAMRA-3′.

Primary screening assay and secondary confirmation assay. HCoV-OC43 can replicate efficiently in BHK-21 cells, with this cell line commonly used for virus isolation or antiviral screening assays. Therefore, the primary screening assay was conducted using 10 μM each compound in BHK-21 cells. We observed no difference in the average Rluc signal between mock controls (only reporter virus added) and DMSO controls. The average control (mock or DMSO control) signal was $\sim$6.3 $\times$ 10^6 luciferase light units, and that for the background (only BHK-21 cells) was $\sim$25 luciferase light units.

Briefly, $\sim$4,000 BHK-21 cells were seeded on 96-well plates in DMEM supplemented with 10% FBS. After overnight incubation in a 5% CO_2 atmosphere at 37°C, each well contained $\sim$10,000 cells. The medium was then replaced with 94 μl DMEM supplemented with 3% FBS, and 1 μl of each compound (diluted in DMSO) was added to the plates at a final concentration of 10 μM (one compound per well) in triplicate. An equal volume of DMSO alone was added to the DMSO control wells (Fig. 1A). After incubation for 60 min, 5 μl of diluted viral suspension was added to each well (MOI = 0.01) for a final total screening volume of 100 μl/well. The plates were incubated at 37°C for 72 h, and luciferase activity was determined using the Renilla-Glo luciferase assay system (Promega, Madison, WI, USA) according to the manufacturer's instructions. Antiviral activity was calculated as follows: inhibition of Rluc activity (%) = 100% − (relative luminescence units of compound-treated cells/relative luminescence units of DMSO-treated control cells). Cytotoxicity was calculated as follows: inhibition of BHK-21 proliferation (%) = 100% − (cell viability of compound-treated cells/cell viability of DMSO-treated control cells). The EC_{50} value and the compound-specific toxicity (CC_{50}) were calculated with GraphPad Prism 5 software (GraphPad, Inc., La Jolla, CA, USA) using the nonlinear regression model. The Z factor, an assessment of the quality of screening assays, was determined, and compounds were considered effective if they reduced Rluc activity by $\geq$70% and cytotoxicity by $\leq$80%.

A confirmation assay was performed using HCoV-OC43-WT treated with the compounds at two concentrations (10 and 5 μM), and viral RNA load was determined by qRT-PCR. To screen hits with higher potency and narrow the screening scope, a compound was considered effective only if the EC_{50} value was $<$5 μM.

Western blot analysis. BHK-21 cells were lysed by incubation in 0.5% NP-40 buffer for 30 min at 4°C. Lysates were separated by sodium dodecyl sulfate-polyacrylamide gel electrophoresis and transferred to nitrocellulose membranes, which were blocked with 5% skim milk in PBS for 1 h and incubated with the primary antibody overnight at 4°C. After washing with PBS plus Tween 20 buffer, the membranes were incubated for 1 h with the appropriate secondary antibody and scanned using the Odyssey Infrared imaging system (LI-COR Biosciences).

IFA. BHK-21 cells in 96-well plates were infected with HCoV-OC43-WT (MOI = 0.01) in the presence of 10 μM the indicated inhibitors, with chloroquine and DMSO used as the positive and negative controls, respectively. At 72 h postinfection, cells were fixed in 4% formaldehyde, permeabilized in 0.5% Triton X-100, blocked in 5% bovine serum albumin in PBS, and then probed with primary antibodies (anti-HCoV-OC43 nucleocapsid protein) for 1 h at room temperature. The cells were washed three times with PBS and then incubated with fluorescein isothiocyanate-labeled goat anti-mouse IgG (Sigma-Aldrich, St. Louis, MO, USA) at a dilution of 1:100 for 1 h. The cells were then washed and stained with 4,6-diamidino-2-phenylindole (DAPI; Invitrogen, Carlsbad, CA, USA) to detect nuclei. Fluorescence images were obtained and analyzed using a fluorescence microscope (TE2000U; Nikon, Melville, NY, USA) with a video documentation system.

Cell viability assay. Cell viability was assessed by a methyl-thiazolyl-tetrazolium (MTT) assay. After 72 h, MTT was added to a final concentration of 0.5 mg/ml, and cells were incubated for 3 h in a humidified 5% CO_2 incubator at 37°C. The plates were then centrifuged (500 $\times$ *g*, 10 min), and the supernatant was removed from each well by aspiration with a micropipette. Subsequently, 100 μl of DMSO was added per well, and the plates were gently shaken. The absorbance at 580 nm was detected using a Microelisa Auto Reader MR580 spectrometer (Dynatech Laboratories, Inc., Charlottesville, VA, USA).

MERS-CoV entry inhibition assay. The inhibitory activity of the selected inhibitors on CoV entry was determined using pseudoviruses, as described previously (41). Briefly, 293FT cells were cotransfected with plasmids PNL4-3.luc.RE- and pVRC-MERS-S, and the culture supernatant containing sufficient pseudotyped MERS-CoV was collected at 72 h posttransfection. Upon reaching a density of 5,000 cells/well in a 96-well plate, dipeptidyl peptidase 4 (DPP4)-expressing Huh7.5 cells were infected with 200 $TCID_{50}$ of the pseudovirus MERS-CoV in the presence of each inhibitor at different concentrations. The culture medium was renewed with fresh medium containing 2% FBS, and luciferase activity was determined after an additional 48 h of incubation using a Promega GloMax 96 plate luminometer (Promega).

Mice and infection. Twelve-day-old female BALB/c mice were inoculated via the intranasal route with 100 $TCID_{50}$ HCoV-OC43-WT or rOC43-ns2Del-Rluc. After 2 h, the mice were treated with the test compounds in 1$\times$ DMSO and PBS buffer. The animals were injected intraperitoneally daily with 10 μl of the compounds (emetine was used at 5 mg/kg, chloroquine was used at 30 mg/kg, and other inhibitors were used at 15 mg/kg), and survival was monitored for 20 days postinoculation. All procedures involving animals were performed in compliance with the Guide for the Care and Use of Laboratory Animals of the People's Republic of China. The study protocol was approved by the Committee on the Ethics of Animal Experiments of the Chinese Center for Disease Control and Prevention.

BLI. BALB/c mice were infected with rOC43-ns2Del-Rluc and treated with lycorine or DMSO-PBS, followed by immediate anesthetization with 2% isoflurane and intraperitoneal administration of ViviRen *in vivo Renilla* luciferase substrate (20 μg/g; Promega) at 2, 3, and 4 days postinoculation. The mice were positioned in a specially designed box and placed onto the stage inside the light-tight camera box. Mice

were imaged within 5 min postinjection of the substrate, and photon flux was quantitated using Living Image software (PerkinElmer, Waltham, MA, USA).

IHC. Mouse brains were removed at 3 days postinfection and fixed in formalin, and the tissues were processed for IHC, as described previously (66).

Statistical analysis. Differences between groups were examined for statistical significance using Student's *t* test. A *P* of <0.05 was considered statistically significant.

SUPPLEMENTAL MATERIAL

Supplemental material for this article may be found at https://doi.org/10.1128/JVI.00023-19.

SUPPLEMENTAL FILE 1, XLS file, 0.5 MB.

ACKNOWLEDGMENTS

We thank P. J. Talbot (INRS-Institute Armand-Frappier, Université du Québec, Laval, Québec, Canada) for providing the infectious clone of HCoV-OC43 (WT), Bart L. Haagmans and Ron A. M. Fouchier (Erasmus MC, Rotterdam, the Netherlands) for providing MERS-CoV (isolate hCoV-EMC/2012), Lia van der Hoek (Center for Infection and Immunity Amsterdam, Academic Medical Center, University of Amsterdam, the Netherlands) for providing HCoV-NL63 strain Amsterdam I, and Hongyu Deng (CAS Key Laboratory of Infection and Immunity, Institute of Biophysics, Chinese Academy of Sciences) for providing MHV strain A59.

This work was supported by the National Key Research and Development Program of China (grant 2016YFD0500300 to W.T. and grant 2016YFC1200200 to B.H.) and by the Megaproject for Infectious Disease Research of China (grant 2016ZX10004001-003 to W.T.).

The funders had no role in the study design, data collection and analysis, decision to publish, or preparation of the manuscript.

We have submitted the ICMJE Form for Disclosure of Potential Conflicts of Interest. Conflicts that the editors consider relevant to the content of the manuscript have been disclosed.

L.S. and W.T. designed the study and wrote the first draft of the manuscript. L.S., J.N., C.W., B.H., W.W., N.Z., Y.D., H.W., and F.Y. conducted the experiments. L.S. conducted the statistical analysis. L.S., S.C., and W.T. performed data interpretation. B.H. and W.T. supervised the project.

The findings and conclusions in this report are those of the authors and do not necessarily represent the official position of the China CDC.

REFERENCES

1. Saberi A, Gulyaeva AA, Brubacher JL, Newmark PA, Gorbalenya AE. 2018. A planarian nidovirus expands the limits of RNA genome size. PLoS Pathog 14:e1007314. https://doi.org/10.1371/journal.ppat.1007314.
2. Woo PC, Lau SK, Huang Y, Yuen KY. 2009. Coronavirus diversity, phylogeny and interspecies jumping. Exp Biol Med (Maywood) 234:1117–1127. https://doi.org/10.3181/0903-MR-94.
3. Zaki AM, van Boheemen S, Bestebroer TM, Osterhaus AD, Fouchier RA. 2012. Isolation of a novel coronavirus from a man with pneumonia in Saudi Arabia. N Engl J Med 367:1814–1820. https://doi.org/10.1056/NEJMoa1211721.
4. Eckerle LD, Becker MM, Halpin RA, Li K, Venter E, Lu X, Scherbakova S, Graham RL, Baric RS, Stockwell TB, Spiro DJ, Denison MR. 2010. Infidelity of SARS-CoV Nsp14-exonuclease mutant virus replication is revealed by complete genome sequencing. PLoS Pathog 6:e1000896. https://doi.org/10.1371/journal.ppat.1000896.
5. Pyrc K, Dijkman R, Deng L, Jebbink MF, Ross HA, Berkhout B, van der Hoek L. 2006. Mosaic structure of human coronavirus NL63, one thousand years of evolution. J Mol Biol 364:964–973. https://doi.org/10.1016/j.jmb.2006.09.074.
6. Su S, Wong G, Shi W, Liu J, Lai ACK, Zhou J, Liu W, Bi Y, Gao GF. 2016. Epidemiology, genetic recombination, and pathogenesis of coronaviruses. Trends Microbiol 24:490–502. https://doi.org/10.1016/j.tim.2016.03.003.
7. de Wit E, van Doremalen N, Falzarano D, Munster VJ. 2016. SARS and MERS: recent insights into emerging coronaviruses. Nat Rev Microbiol 14:523–534. https://doi.org/10.1038/nrmicro.2016.81.
8. Müller MA, Meyer B, Corman VM, Al-Masri M, Turkestani A, Ritz D, Sieberg A, Aldabbagh S, Bosch BJ, Lattwein E, Alhakeem RF, Assiri AM, Albarrak AM, Al-Shangiti AM, Al-Tawfiq JA, Wikramaratna P, Alrabeeah AA, Drosten C, Memish ZA. 2015. Presence of Middle East respiratory syndrome coronavirus antibodies in Saudi Arabia: a nationwide, cross-sectional, serological study. Lancet Infect Dis 15:559–564. https://doi.org/10.1016/S1473-3099(15)70090-3.
9. Loutfy MR, Blatt LM, Siminovitch KA, Ward S, Wolff B, Lho H, Pham DH, Deif H, LaMere EA, Chang M, Kain KC, Farcas GA, Ferguson P, Latchford M, Levy G, Dennis JW, Lai EK, Fish EN. 2003. Interferon alfacon-1 plus corticosteroids in severe acute respiratory syndrome: a preliminary study. JAMA 290:3222–3228. https://doi.org/10.1001/jama.290.24.3222.
10. Lee N, Hui D, Wu A, Chan P, Cameron P, Joynt GM, Ahuja A, Yung MY, Leung CB, To KF, Lui SF, Szeto CC, Chung S, Sung JJ. 2003. A major outbreak of severe acute respiratory syndrome in Hong Kong. N Engl J Med 348:1986–1994. https://doi.org/10.1056/NEJMoa030685.
11. Shalhoub S, Farahat F, Al-Jiffri A, Simhairi R, Shamma O, Siddiqi N, Siddiqi N, Mushtaq A. 2015. IFN-α2a or IFN-β1a in combination with ribavirin to treat Middle East respiratory syndrome coronavirus pneumonia: a retrospective study. J Antimicrob Chemother 70:2129–2132. https://doi.org/10.1093/jac/dkv085.

12. Booth CM, Matukas LM, Tomlinson GA, Rachlis AR, Rose DB, Dwosh HA, Walmsley SL, Mazzulli T, Avendano M, Derkach P, Ephtimios IE, Kitai I, Mederski BD, Shadowitz SB, Gold WL, Hawryluck LA, Rea E, Chenkin JS, Cescon DW, Poutanen SM, Detsky AS. 2003. Clinical features and short-term outcomes of 144 patients with SARS in the greater Toronto area. JAMA 289:2801–2809. https://doi.org/10.1001/jama.289.21.JOC30885.
13. Zumla A, Chan JF, Azhar EI, Hui DS, Yuen KY. 2016. Coronaviruses—drug discovery and therapeutic options. Nat Rev Drug Discov 15:327–347. https://doi.org/10.1038/nrd.2015.37.
14. de Wilde AH, Jochmans D, Posthuma CC, Zevenhoven-Dobbe JC, van Nieuwkoop S, Bestebroer TM, van den Hoogen BG, Neyts J, Snijder EJ. 2014. Screening of an FDA-approved compound library identifies four small-molecule inhibitors of Middle East respiratory syndrome coronavirus replication in cell culture. Antimicrob Agents Chemother 58:4875–4884. https://doi.org/10.1128/AAC.03011-14.
15. Dyall J, Coleman CM, Hart BJ, Venkataraman T, Holbrook MR, Kindrachuk J, Johnson RF, Olinger GG, Jr, Jahrling PB, Laidlaw M, Johansen LM, Lear-Rooney CM, Glass PJ, Hensley LE, Frieman MB. 2014. Repurposing of clinically developed drugs for treatment of Middle East respiratory syndrome coronavirus infection. Antimicrob Agents Chemother 58:4885–4893. https://doi.org/10.1128/AAC.03036-14.
16. Müller C, Schulte FW, Lange-Grünweller K, Obermann W, Madhugiri R, Pleschka S, Ziebuhr J, Hartmann RK, Grünweller A. 2018. Broad-spectrum antiviral activity of the eIF4A inhibitor silvestrol against corona- and picornaviruses. Antiviral Res 150:123–129. https://doi.org/10.1016/j.antiviral.2017.12.010.
17. Sheahan TP, Sims AC, Graham RL, Menachery VD, Gralinski LE, Case JB, Leist SR, Pyrc K, Feng JY, Trantcheva I, Bannister R, Park Y, Babusis D, Clarke MO, Mackman RL, Spahn JE, Palmiotti CA, Siegel D, Ray AS, Cihlar T, Jordan R, Denison MR, Baric RS. 2017. Broad-spectrum antiviral GS-5734 inhibits both epidemic and zoonotic coronaviruses. Sci Transl Med 9:eaal3653. https://doi.org/10.1126/scitranslmed.aal3653.
18. Shen L, Yang Y, Ye F, Liu G, Desforges M, Talbot PJ, Tan W. 2016. Safe and sensitive antiviral screening platform based on recombinant human coronavirus OC43 expressing the luciferase reporter gene. Antimicrob Agents Chemother 60:5492–5503. https://doi.org/10.1128/AAC.00814-16.
19. Evidente A, Cicala MR, Giudicianni I, Randazzo G, Riccio R. 1983. 1H and 13C NMR analysis of lycorine and α-dihydrolycorine. Phytochemistry 22:581–584. https://doi.org/10.1016/0031-9422(83)83051-9.
20. Liu R, Cao Z, Tu J, Pan Y, Shang B, Zhang G, Bao M, Zhang S, Yang P, Zhou Q. 2012. Lycorine hydrochloride inhibits metastatic melanoma cell-dominant vasculogenic mimicry. Pigment Cell Melanoma Res 25:630–638. https://doi.org/10.1111/j.1755-148X.2012.01036.x.
21. Cho N, Du Y, Valenciano AL, Fernández-Murga ML, Goetz M, Clement J, Cassera MB, Kingston D. 2018. Antiplasmodial alkaloids from bulbs of Amaryllis belladonna Steud. Bioorg Med Chem Lett 28:40–42. https://doi.org/10.1016/j.bmcl.2017.11.021.
22. Bendaif H, Melhaoui A, Ramdani M, Elmsellem H, Douez C, El Ouadi Y. 2018. Antibacterial activity and virtual screening by molecular docking of lycorine from Pancratium foetidum Pom (Moroccan endemic Amaryllidaceae). Microb Pathog 115:138–145. https://doi.org/10.1016/j.micpath.2017.12.037.
23. Chen S, Fang XQ, Zhang JF, Ma Y, Tang XZ, Zhou ZJ, Wang JY, Qin A, Fan SW. 2016. Lycorine protects cartilage through suppressing the expression of matrix metalloprotenases in rat chondrocytes and in a mouse osteoarthritis model. Mol Med Rep 14:3389–3396. https://doi.org/10.3892/mmr.2016.5594.
24. Xu W, Lacerda L, Debeb BG, Atkinson RL, Solley TN, Li L, Orton D, McMurray JS, Hang BI, Lee E, Klopp AH, Ueno NT, Reuben JM, Krishnamurthy S, Woodward WA. 2013. The antihelmintic drug pyrvinium pamoate targets aggressive breast cancer. PLoS One 8:e71508. https://doi.org/10.1371/journal.pone.0071508.
25. Keyaerts E, Li S, Vijgen L, Rysman E, Verbeeck J, Van Ranst M, Maes P. 2009. Antiviral activity of chloroquine against human coronavirus OC43 infection in newborn mice. Antimicrob Agents Chemother 53:3416–3421. https://doi.org/10.1128/AAC.01509-08.
26. Jacomy H, Talbot PJ. 2003. Vacuolating encephalitis in mice infected by human coronavirus OC43. Virology 315:20–33. https://doi.org/10.1016/S0042-6822(03)00323-4.
27. St-Jean JR, Jacomy H, Desforges M, Vabret A, Freymuth F, Talbot PJ. 2004. Human respiratory coronavirus OC43: genetic stability and neuroinvasion. J Virol 78:8824–8834. https://doi.org/10.1128/JVI.78.16.8824-8834.2004.
28. Morfopoulou S, Brown JR, Davies EG, Anderson G, Virasami A, Qasim W, Chong WK, Hubank M, Plagnol V, Desforges M, Jacques TS, Talbot PJ, Breuer J. 2016. Human coronavirus OC43 associated with fatal encephalitis. N Engl J Med 375:497–498. https://doi.org/10.1056/NEJMc1509458.
29. Yeh EA, Collins A, Cohen ME, Duffner PK, Faden H. 2004. Detection of coronavirus in the central nervous system of a child with acute disseminated encephalomyelitis. Pediatrics 113:e73–e76.
30. Cheng VC, Lau SK, Woo PC, Yuen KY. 2007. Severe acute respiratory syndrome coronavirus as an agent of emerging and reemerging infection. Clin Microbiol Rev 20:660–694. https://doi.org/10.1128/CMR.00023-07.
31. Chan JF, Lau SK, To KK, Cheng VC, Woo PC, Yuen KY. 2015. Middle East respiratory syndrome coronavirus: another zoonotic betacoronavirus causing SARS-like disease. Clin Microbiol Rev 28:465–522. https://doi.org/10.1128/CMR.00102-14.
32. Zumla A, Hui DS, Perlman S. 2015. Middle East respiratory syndrome. Lancet 386:995–1007. https://doi.org/10.1016/S0140-6736(15)60454-8.
33. Falzarano D, de Wit E, Martellaro C, Callison J, Munster VJ, Feldmann H. 2013. Inhibition of novel β coronavirus replication by a combination of interferon-α2b and ribavirin. Sci Rep 3:1686. https://doi.org/10.1038/srep01686.
34. Hart BJ, Dyall J, Postnikova E, Zhou H, Kindrachuk J, Johnson RF. 2014. Interferon-β and mycophenolic acid are potent inhibitors of Middle East respiratory syndrome coronavirus in cell-based assays. J Gen Virol 9:571–577. https://doi.org/10.1099/vir.0.061911-0.
35. Yamamoto N, Yang R, Yoshinaka Y, Amari S, Nakano T, Cinatl J, Rabenau H, Doerr HW, Hunsmann G, Otaka A, Tamamura H, Fujii N, Yamamoto N. 2004. HIV protease inhibitor nelfinavir inhibits replication of SARS-associated coronavirus. Biochem Biophys Res Commun 18:719–725. https://doi.org/10.1016/j.bbrc.2004.04.083.
36. Chan JF, Chan KH, Kao RY, To KK, Zheng BJ, Li CP, Li PT, Dai J, Mok FK, Chen H, Hayden FG, Yuen KY. 2013. Broad-spectrum antivirals for the emerging Middle East respiratory syndrome coronavirus. J Infect 67:606–616. https://doi.org/10.1016/j.jinf.2013.09.029.
37. Shin JS, Jung E, Kim M, Baric RS, Go YY. 2018. Saracatinib inhibits Middle East respiratory syndrome-coronavirus replication in vitro. Viruses 10:pii: E283. https://doi.org/10.3390/v10060283.
38. Rabaan AA, Alahmed SH, Bazzi AM, Alhani HM. 2017. A review of candidate therapies for Middle East respiratory syndrome from a molecular perspective. J Med Microbiol 66:1261–1274. https://doi.org/10.1099/jmm.0.000565.
39. Agostini ML, Andres EL, Sims AC, Graham RL, Sheahan TP, Lu X, Smith EC, Case JB, Feng JY, Jordan R, Ray AS, Cihlar T, Siegel D, Mackman RL, Clarke MO, Baric RS, Denison MR. 2018. Coronavirus susceptibility to the antiviral remdesivir (GS-5734) is mediated by the viral polymerase and the proofreading exoribonuclease. mBio 9:e00221-18.
40. Channappanavar R, Lu L, Xia S, Du L, Meyerholz DK, Perlman S, Jiang S. 2015. Protective effect of intranasal regimens containing peptidic Middle East respiratory syndrome coronavirus fusion inhibitor against MERS-CoV infection. J Infect Dis 212:1894–1903. https://doi.org/10.1093/infdis/jiv325.
41. Niu P, Zhang S, Zhou P, Huang B, Deng Y, Qin K, Wang P, Wang W, Wang X, Zhou J, Zhang L, Tan W. 2018. Ultra-potent human neutralizing antibody repertoires against MERS-CoV from a recovered patient. J Infect Dis 218:1249–1260. https://doi.org/10.1093/infdis/jiy311.
42. Jiang L, Wang N, Zuo T, Shi X, Poon KM, Wu Y, Gao F, Li D, Wang R, Guo J, Fu L, Yuen KY, Zheng BJ, Wang X, Zhang L. 2014. Potent neutralization of MERS-CoV by human neutralizing monoclonal antibodies to the viral spike glycoprotein. Sci Transl Med 6:234.
43. Lamoral-Theys D, Decaestecker C, Mathieu V, Dubois J, Kornienko A, Kiss R, Evidente A, Pottier L. 2010. Lycorine and its derivatives for anticancer drug design. Mini Rev Med Chem 10:41–50. https://doi.org/10.2174/138955710791112604.
44. Cedrón JC, Gutiérrez D, Flores N, Ravelo AG, Estévez-Braun A. 2010. Synthesis and antiplasmodial activity of lycorine derivatives. Bioorg Med Chem 18:4694–4701. https://doi.org/10.1016/j.bmc.2010.05.023.
45. Toriizuka Y, Kinoshita E, Kogure N, Kitajima M, Ishiyama A, Otoguro K, Yamada H, Omura S, Takayama H. 2008. New lycorine-type alkaloid from Lycoris traubii and evaluation of antitrypanosomal and antimalarial activities of lycorine derivatives. Bioorg Med Chem 16:10182–10189. https://doi.org/10.1016/j.bmc.2008.10.061.
46. Hwang YC, Chu JJ, Yang PL, Chen W, Yates MV. 2008. Rapid identification of inhibitors that interfere with poliovirus replication using a cell-based assay. Antiviral Res 77:232–236. https://doi.org/10.1016/j.antiviral.2007.12.009.
47. Li B, Wang Q, Pan X, Fernández de Castro I, Sun Y, Guo Y, Tao X, Risco

C, Sui SF, Lou Z. 2013. Bunyamwera virus possesses a distinct nucleocapsid protein to facilitate genome encapsidation. Proc Natl Acad Sci U S A 110:9048–9053. https://doi.org/10.1073/pnas.1222552110.
48. Gabrielsen B, Monath TP, Huggins JW, Kefauver DF, Pettit GR, Groszek G, Hollingshead M, Kirsi JJ, Shannon WM, Schubert EM, DaRe J, Ugarkar B, Ussery MA, Phelan MJ. 1992. Antiviral (RNA) activity of selected Amaryllidaceae isoquinoline constituents and synthesis of related substances. J Nat Prod 55:1569–1581. https://doi.org/10.1021/np50089a003.
49. Li SY, Chen C, Zhang HQ, Guo HY, Wang H, Wang L, Zhang X, Hua SN, Yu J, Xiao PG, Li RS, Tan X. 2005. Identification of natural compounds with antiviral activities against SARS-associated coronavirus. Antiviral Res 67:18–23. https://doi.org/10.1016/j.antiviral.2005.02.007.
50. Liu J, Yang Y, Xu Y, Ma C, Qin C, Zhang L. 2011. Lycorine reduces mortality of human enterovirus 71-infected mice by inhibiting virus replication. Virol J 8:483. https://doi.org/10.1186/1743-422X-8-483.
51. Guo Y, Wang Y, Cao L, Wang P, Qing J, Zheng Q, Shang L, Yin Z, Sun Y. 2016. A conserved inhibitory mechanism of a lycorine derivative against enterovirus and hepatitis C virus. Antimicrob Agents Chemother 60:913–924. https://doi.org/10.1128/AAC.02274-15.
52. He J, Qi WB, Wang L, Tian J, Jiao PR, Liu GQ, Ye WC, Liao M. 2013. Amaryllidaceae alkaloids inhibit nuclear-to-cytoplasmic export of ribonucleoprotein (RNP) complex of highly pathogenic avian influenza virus H5N1. Influenza Other Respir Viruses 7:922–931. https://doi.org/10.1111/irv.12035.
53. Matthews H, Usman-Idris M, Khan F, Read M, Nirmalan N. 2013. Drug repositioning as a route to anti-malarial drug discovery: preliminary investigation of the in vitro anti-malarial efficacy of emetine dihydrochloride hydrate. Malar J 12:359. https://doi.org/10.1186/1475-2875-12-359.
54. Low JSY, Chen KC, Wu KX, Ng ML, Chu JJH. 2009. Antiviral activity of emetine dihydrochloride against dengue virus infection. J Antivirals & Antiretrovirals 1:62–71.
55. Chaves Valadão AL, Abreu CM, Dias JZ, Arantes P, Verli H, Tanuri A, de Aguiar RS. 2015. Natural plant alkaloid (emetine) inhibits HIV-1 replication by interfering with reverse transcriptase activity. Molecules 20:11474–11489. https://doi.org/10.3390/molecules200611474.
56. Khandelwal N, Chander Y, Rawat KD, Riyesh T, Nishanth C, Sharma S, Jindal N, Tripathi BN, Barua S, Kumar N. 2017. Emetine inhibits replication of RNA and DNA viruses without generating drug-resistant virus variants. Antiviral Res 144:196–204. https://doi.org/10.1016/j.antiviral.2017.06.006.
57. MacGibeny MA, Koyuncu OO, Wirblich C, Schnell MJ, Enquist LW. 2018. Retrograde axonal transport of rabies virus is unaffected by interferon treatment but blocked by emetine locally in axons. PLoS Pathog 14:e1007188. https://doi.org/10.1371/journal.ppat.1007188.
58. Mukhopadhyay R, Roy S, Venkatadri R, Su YP, Ye W, Barnaeva E, Mathews Griner L, Southall N, Hu X, Wang AQ, Xu X, Dulcey AE, Marugan JJ, Ferrer M, Arav-Boger R. 2016. Efficacy and mechanism of action of low dose emetine against human cytomegalovirus. PLoS Pathog 12:e1005717. https://doi.org/10.1371/journal.ppat.1005717.
59. Yang S, Xu M, Lee EM, Gorshkov K, Shiryaev SA, He S, Sun W, Cheng YS, Hu X, Tharappel AM, Lu B, Pinto A, Farhy C, Huang CT, Zhang Z, Zhu W, Wu Y, Zhou Y, Song G, Zhu H, Shamim K, Martínez-Romero C, García-Sastre A, Preston RA, Jayaweera DT, Huang R, Huang W, Xia M, Simeonov A, Ming G, Qiu X, Terskikh AV, Tang H, Song H, Zheng W. 2018. Emetine inhibits Zika and Ebola virus infections through two molecular mechanisms: inhibiting viral replication and decreasing viral entry. Cell Discov 4:31. https://doi.org/10.1038/s41421-018-0034-1.
60. Chan JF, Yao Y, Yeung ML, Deng W, Bao L, Jia L, Li F, Xiao C, Gao H, Yu P, Cai JP, Chu H, Zhou J, Chen H, Qin C, Yuen KY. 2015. Treatment with lopinavir/ritonavir or interferon-β1b improves outcome of MERS-CoV infection in a nonhuman primate model of common marmoset. J Infect Dis 212:1904–1913. https://doi.org/10.1093/infdis/jiv392.
61. Alonso-Caplen FV, Matsuoka Y, Wilcox GE, Compans RW. 1984. Replication and morphogenesis of avian coronavirus in Vero cells and their inhibition by monensin. Virus Res 1:153–167. https://doi.org/10.1016/0168-1702(84)90070-4.
62. Niemann H, Boschek B, Evans D, Rosing M, Tamura T, Klenk HD. 1982. Post-translational glycosylation of coronavirus glycoprotein E1: inhibition by monensin. EMBO J 1:1499–1504. https://doi.org/10.1002/j.1460-2075.1982.tb01346.x.
63. Kim JC, Spence RA, Currier PF, Lu X, Denison MR. 1995. Coronavirus protein processing and RNA synthesis is inhibited by the cysteine proteinase inhibitor e64dd. Virology 208:1–8. https://doi.org/10.1006/viro.1995.1123.
64. Lu R, Yu X, Wang W, Duan X, Zhang L, Zhou W, Xu J, Xu L, Hu Q, Lu J, Ruan L, Wang Z, Tan W. 2012. Characterization of human coronavirus etiology in Chinese adults with acute upper respiratory tract infection by real-time RT-PCR assays. PLoS One 7:e38638. https://doi.org/10.1371/journal.pone.0038638.
65. Corman VM, Müller MA, Costabel U, Timm J, Binger T, Meyer B, Kreher P, Lattwein E, Eschbach-Bludau M, Nitsche A, Bleicker T, Landt O, Schweiger B, Drexler JF, Osterhaus AD, Haagmans BL, Dittmer U, Bonin F, Wolff T, Drosten C. 2012. Assays for laboratory confirmation of novel human coronavirus (hCoV-EMC) infections. Euro Surveill 17:20334.
66. Lan J, Yao Y, Deng Y, Chen H, Lu G, Wang W, Bao L, Deng W, Wei Q, Gao GF, Qin C, Tan W. 2015. Recombinant receptor binding domain protein induces partial protective immunity in rhesus macaques against Middle East respiratory syndrome coronavirus challenge. EBioMedicine 2:1438–1446. https://doi.org/10.1016/j.ebiom.2015.08.031.